The development of grain-orientation-dependent residual stressess in a cyclically deformed alloy

YAN-DONG WANG*[1], HONGBO TIAN[2], ALEXANDRU D. STOICA[1], XUN-LI WANG*[1,3], PETER K. LIAW[2] AND JAMES W. RICHARDSON[4]

[1]Spallation Neutron Source, Oak Ridge National Laboratory, Oak Ridge, Tennessee 37830, USA
[2]Department of Materials Science and Engineering, The University of Tennessee, Knoxville, Tennessee 37996-2200, USA
[3]Metals and Ceramics Division, Oak Ridge National Laboratory, Oak Ridge, Tennessee 37831, USA
[4]Intense Pulsed Neutron Source, Argonne National Laboratory, Argonne, Illinois 60439, USA
*e-mail: wangy@ornl.gov, wangxl@ornl.gov

Published online: 19 January 2003; doi:10.1038/nmat812

There have been numerous efforts to understand and control the resistance of materials to fracture by repeated or cyclic stresses. The micromechanical behaviours, particularly the distributions of stresses on the scale of grain size during or after mechanical or electrical fatigue, are crucial to a full understanding of the damage mechanisms in these materials. Whether a large microstress develops during cyclic deformation with a small amount of monotonic strain but a large amount of accumulated strain remains an open question. Here, we report a neutron diffraction investigation of the development of intergranular stresses, which vary as a function of grain orientations, in 316 stainless steel during high-cycle fatigue. We found that a large intergranular stress developed before cracks started to appear. With further increase of fatigue cycles, the intergranular stress decreased, while the elastic intragranular stored energy continued to grow. One implication of our findings is that the ratio between the intergranular and intragranular stored energies during various stages of fatigue deformation may validate the damage mechanism and can be used as a fingerprint for monitoring the state of fatigue damage in materials.

Most metals, ceramics, or natural rocks are aggregates of crystalline grains with their own characteristic crystallographic orientations (or grain orientations) measured in the sample coordinate system. When a polycrystalline material is deformed, not only macrostresses (average stresses over a certain gauge volume) but also microstresses are produced. The latter include intergranular stresses that vary over the size of grains, as well as the intragranular stresses located around the crystallographic defects. The existence of intergranular stresses in single-phase materials is due to the discontinuity of the stress distribution from grain to grain, caused by so-called elastic or/and plastic incompatibility, which has been investigated by 3D plasticity modelling[1–3] in combination with lattice strain measurements by neutron diffraction. Although there have been extensive studies of the mechanisms of grain-to-grain interactions during the monotonic deformation, investigations on the micromechanical behaviour during or after cyclic loading have just begun[4,5] and the results are far from being understood. A main difficulty in the study of grain-to-grain interactions during cyclic deformations by theoretical simulations is that the microhardening behaviour due to alternating stresses may be not the same as in monotonic stresses. Furthermore, quantitative models that can describe the influence of the microcracks produced during cyclic loading are still lacking. Thus, first-hand experimental investigations on microstress distributions in fatigued materials and how they develop are essential for answering some of the fundamental questions in fatigue, such as whether there exists a correlation between the intergranular stresses and the damage mechanisms.

Synchrotron-based microbeam X-ray diffraction is a promising way for direct measurement of the strain or stress states of individual grains during cyclic deformation[6,7]. However, in order to describe the properties of polycrystalline aggregates, it is necessary to measure the stress distribution for a large number of individual grains with reliable statistics. Despite recent advances in synchrotron techniques, mapping the local strains in materials with a fine subgrain structure induced by deformation is still a challenge. An alternative method is to use high-energy X-rays or neutrons to determine the strain distributions of specific lattice planes with respect to the sample

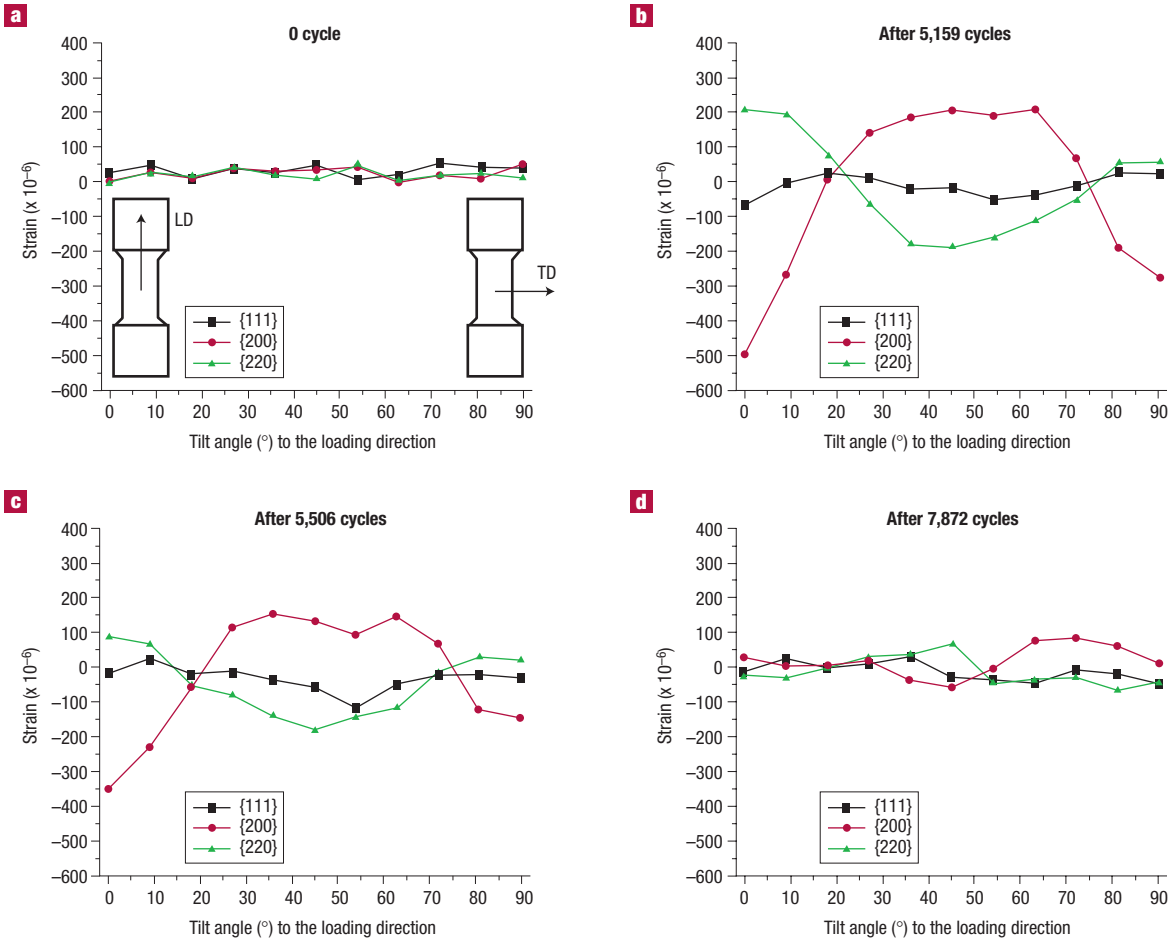

Figure 1 Lattice strain distributions in the 316 stainless steel obtained with {111}, {200}, and {220} reflections as a function of tilt angle relative to the loading direction (LD) at different stages of fatigue. **a**, 0 cycle or virgin sample, **b**, 5,159 cycles (when microcracks start to appear on the surface), **c**, 5,506 cycles (after cracks start to propagate into the bulk), and **d**, 7,872 cycles (after fatigue failure is reached). The differences in orientation dependence are due to the presence of intergranular stress. TD is the transverse direction.

directions over a bulk sample. Although the strain of individual grains cannot be spatially resolved with this technique, a statistical distribution of the strain/stress as a function of the grain orientations can be established from the experimental strain data[8–10]. We have named this kind of stress as the grain-orientation-dependent stress and the stress distribution as the stress orientation distribution function or SODF. In this concept, the grain-orientation-dependent intergranular stress is resolved in the (Euler) orientation space rather than in real space.

Commercial Type 316 stainless steel, a corrosion-resistant alloy widely used in the chemical and nuclear industries, was chosen to study the development of grain-orientation-dependent residual stresses after fatigue loading. This type of stainless steel is also a candidate material for the containers holding the mercury target of the Spallation Neutron Source being constructed at the Oak Ridge National Laboratory in the USA, and so a large amount of fatigue data are available in a variety of test conditions[11–13]. Before fatigue tests, all specimens were annealed at 1,038 °C for 1 h, and cooled to room temperature in air to release the residual stresses produced by hot-deformation and specimen cutting. Neutron diffraction measurements confirmed that the annealed specimens were indeed free of microstresses, because the diffraction peak positions were independent of the grain orientations. High-cycle fatigue tests with a frequency of 0.2 Hz were conducted in air under a load-control mode using an R ratio of -1 ($R = \sigma_{min}/\sigma_{max}$, where σ_{min} and σ_{max} are, respectively, the minimum and maximum applied stress). Four specimens were studied, three of which were cyclically loaded with the stress amplitude of 287 MPa to 5,159, 5,506 and 7,872 cycles, respectively. The fourth specimen was used as a stress-free reference. Metallographic examinations of these samples revealed uniform austenitic grains with annealing twins and no indications of internal microcracks. The three fatigued cycles were chosen to represent different stages of deformation: when cracks start to appear on the specimen surface, after cracks start to propagate into the bulk, and after failure is reached. Cylindrical samples with a length of 8 mm and diameter of 6 mm were cut by electro-discharge machining from the gauge-length sections of the fatigued specimens and used for neutron diffraction measurements.

The lattice strain distributions for a large number of {hkl}-planes in the fatigued samples were measured using the general purpose powder diffractometer[14] (GPPD) at the Intense Pulsed Neutron Source, Argonne National Laboratory, USA. The beam at the sample position was collimated to a size of 12×30 mm^2, and the sample was fully immersed in the beam so that only the intergranular stress was measured. The samples were mounted with their cylindrical axes, which are also the loading direction (LD), in the horizontal scattering plane. The orthogonal direction in the horizontal scattering plane is defined as a transverse direction (TD). The samples were rotated about the vertical

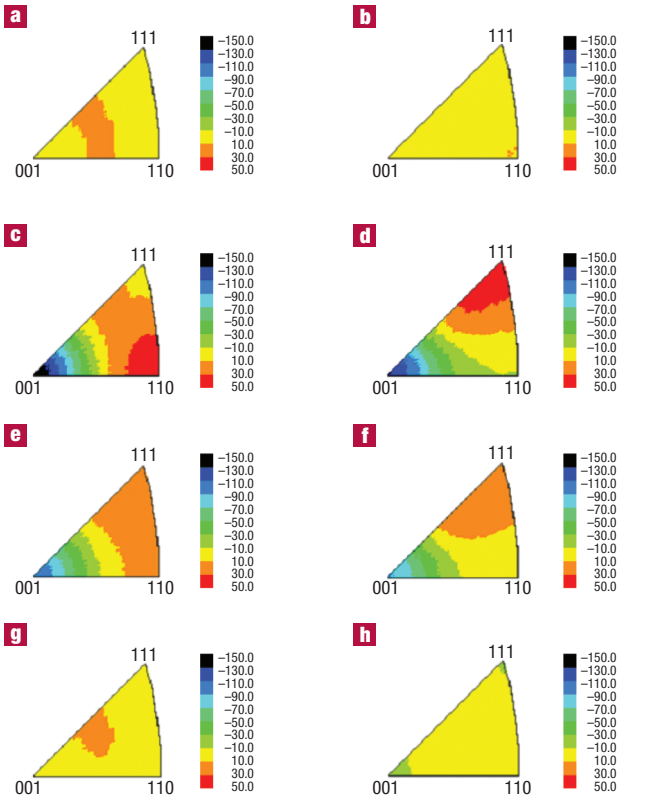

Figure 2 Distributions of residual stresses for various grain orientations in the cyclically deformed 316 stainless steel presented in the form of inverse pole figures. A point <hkl> in the stereographic projection represents grains with <hkl> parallel to LD. The left panel is for stresses along the LD, whereas the right panel is for stresses along TD. (**a,b**) after 0 cycle; (**c,d**) after 5,159 cycles; (**e,f**) after 5,506 cycles; (**g,h**) after 7,872 cycles. The unit of stress is MPa.

Table 1 Measured lattice strains and calculated values from SODF for {111}, {200}, and {220} reflections as a function of tilt angle to the loading direction. The strains are in units of 10^{-6}.

	Tilt angle φ (°)	Lattice strain for {111}		Lattice strain for {200}		Lattice strain for {220}	
		Experiment	Calculated	Experiment	Calculated	Experiment	Calculated
5,159 Cycles	0	−69	−41	−496	−437	210	256
	9	−2	−21	−267	−316	193	219
	18	22	11	2	−75	77	120
	27	10	9	139	86	−62	2
	36	−21	−29	185	124	−178	−83
	45	−18	−60	205	133	−184	−104
	54	−50	−50	189	156	−159	−74
	63	−41	−11	208	116	−108	−28
	72	−10	22	66	−17	−51	13
	81	25	32	−190	−178	57	41
	90	22	32	−276	−250	58	51
5,506 Cycles	0	−21	11	−353	−307	84	119
	9	20	13	−233	−245	68	100
	18	−28	9	−65	−98	−55	53
	27	−19	−11	112	42	−83	−4
	36	−40	−41	151	108	−140	−50
	45	−62	−55	128	107	−182	−68
	54	−122	−37	90	91	−144	−50
	63	−55	0	143	68	−114	−10
	72	−29	28	64	6	−14	28
	81	−25	37	−124	−88	28	48
	90	−32	37	−149	−136	20	53

axis in order to cover all tilt angles from LD to TD in a sequence of measurements, as described previously[15] (see Methods).

The lattice strain distributions obtained with {111}, {200}, and {220} reflections are shown in Fig. 1 as a function of a tilt angle relative to the LD. The nearly zero lattice strains seen in the virgin sample (0 cycle, Fig. 1a) confirmed that the intergranular residual stress in the sample was annealed before fatigue tests. Significant lattice strains were found, however, for samples tested for 5,159 and 5,506 cycles (Fig. 1b,c). In particular, the {200} and {220} lattice strains reverse their signs as the tilt angle changes from 0 (LD) to 90° (TD). These observations gave unambiguous evidence that a large grain-orientation-dependent intergranular stress exists in the 316 stainless steel after high-cycle fatigue. The anisotropy of the lattice strains, which appeared as the amplitude of strain variations for {200} and {220} reflections as a function of the tilt angle, shows an obvious decrease as the number of fatigue cycles is increased to 5,506 (Fig. 1c). When the sample reaches failure after 7,872 cycles, the residual lattice strains for all {hkl} reflections vanish (Fig. 1d).

Cohen *et al.* have investigated the development of intergranular stresses in cyclically deformed alloys since the 1970s[16–9]. They concentrated mainly on the changes of macrostresses in single-phase alloys or phase-stresses in two-phase alloys after fatigue. The {211} reflections in body-centred cubic (b.c.c.) metals or {311} reflections in face-centred cubic (f.c.c.) metals were used for studying the fatigue behaviours due to their relative insensitivities to grain orientations[1–5]. However, although evidence of the grain-orientation-dependent residual stresses was observed by the strong oscillations in the d versus $\sin^2\Psi$ relationship[16], no quantitative information was given on the evolution of those stresses. Here d is the lattice spacing and Ψ the tilt angle of the normal direction of the sample with respect to the scattering vector.

The presence of a large intergranular residual stress prevents the stress values from being reliably evaluated from the measured lattice strains using the conventional stress-analysis technique. Studies[8–10] have established that, just like the crystallographic orientation distribution function, the SODF may be expressed in terms of generalized spherical harmonics, whose series coefficients can be determined directly from the measured lattice strains along various specimen directions. The method to construct the SODF from time-of-flight diffraction data has been published elsewhere[15]. Because the stress or strain distributions of fatigued samples with random grain orientations display axial symmetry around the LD, the SODF representation can be conveniently reduced to a two-dimensional fibre-symmetry group. Thus, although the present SODF was constructed using spherical harmonics up to 8th order, twelve coefficients serve to represent the stress function: they can be uniquely determined by fitting the 60–70 measured lattice strain points. To illustrate the accuracy of the SODF representation, the strain values calculated with SODF are given in Table 1 together with the experimental values. The average difference between the experimental and calculated values is smaller than 50×10^{-6}, which is less than half of the error of typical strain measurements.

The distributions of residual stresses along LD and TD are shown in Fig. 2 in the form of inverse pole figures for various grain orientations (specified by <hkl>||LD in stereographic projection). It can be seen that large grain-orientation-dependent residual stresses developed during fatigue when microcracks start to appear at the sample surface

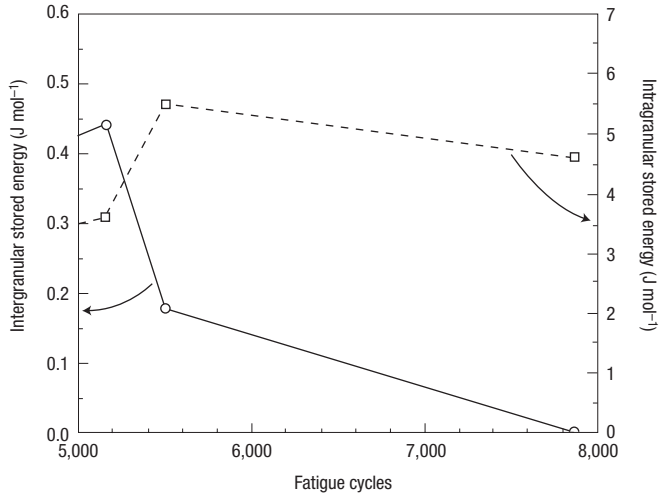

Figure 3 Evolution of intergranular and intragranular stored energies as a function of fatigue cycles. Solid line: intergranular stored energy for grains with <001>||LD. Dashed line: average intragranular stored energy. Because <001>||LD grains show the largest residual stresses, the intergranular stored energy presented here should be considered as an upper bound.

(5,159 cycles, Fig. 2c,d). For stress along the LD, the difference between <001>||LD and <110>||LD grains is about 200 MPa. In addition, a hydrostatic compressive stress is evident for <001>||LD grains, which is compensated in the LD by <110>||LD grains and in the TD by <111>||LD grains. As the microcracks start to propagate into the bulk (5,506 cycles, Fig. 2e,f), the grain-orientation anisotropy of the residual stresses become smaller. When the sample reaches failure, the residual stresses almost completely disappear.

Our results on intergranular stresses up to crack nucleation can be compared with those reported by Lorentzen *et al.*[4] for the early stage of cyclic loading (up to eight successive cycles). That work was conducted as a slow cyclic loading test with the goal to observe *in situ* the lattice strain evolution along and perpendicular to the loading direction. The observed lattice strain loops can be understood by considering the formation of an oscillating intergranular stress state reaching its limits when the load vanishes. The residual stress state measured in our experiment corresponds to the intergranular stress developed during the last half cycle, which was always in compression ($R = -1$). From this point of view, our results showing a (200) lattice contraction in both LD and TD (Fig. 1b) are in good agreement with those by Lorentzen *et al.*[4] This special behaviour of <001>||LD grains was first observed[20] in uniaxial tensile tests and explained as a result of the stainless steel elastic anisotropy, which significantly overcomes the effect of plastic anisotropy predicted by the Taylor model of deformation. These ideas were later confirmed by self-consistent modelling[2,4]. However, our SODF derived from the experimental strain data delivers a complete set of intergranular stress values (from LD to TD) that will provide a more rigorous test of deformation models.

The total energy necessary to induce the grain-orientation-dependent elastic deformation state can be evaluated from the SODF. This energy, which we refer to as intergranular stored energy, shows a sharp decrease after the cracks start to appear, long before the failure. To underscore this point, the estimated intergranular stored energy corresponding to <001>||LD grains are shown in Fig. 3. Because <001>||LD grains show the largest residual stresses, the values presented here should be considered as an upper bound of the intergranular stored energy.

The intergranular stress was evaluated as a mean value for all grains with the same orientation in the Euler space. The strain fluctuations about the mean induce the diffraction peak broadening, which also exhibits a grain-orientation dependence. As was generally accepted for heavily deformed materials, the grain substructure, rather than the intergranular strain variation, produces the strain fluctuations[21]. Because crystallographic defects in the stainless steel are mostly dislocations, the broadening of the diffraction peaks comes primarily from the strain field around dislocations. Within this context, the elastic energy stored in the strain field around dislocations, which we refer to as intragranular stored energy, can be defined.

The strain-induced peak broadening was determined from the integral breadth of the diffraction peak profile (see Methods). For a given {hkl} peak, the peak broadening is dependent on sample orientation, but owing to poor statistics in the measurements of the peak integral breadth, only the average values are used in the following analysis. The variation of peak broadening for a given {hkl} may be considered to be resulting from the variation of the dislocation contrast factor[22]. This approach predicts a contrast factor whose {hkl} dependence varies as a function of the elastic anisotropy and dislocation type (screw or edge)[22]. Taking into account the elastic anisotropy of the stainless steel, our experimental peak-broadening data as a function of {hkl} can be explained by considering the edge dislocations as the main component of the grain substructure. This is a reasonable finding, because the immobile dislocation structure that develops during the fatigue tests of f.c.c. metals shows indeed an edge character[23,24].

Using the known contrast factors, the average density of dislocations was estimated from the peak-broadening data and, subsequently, the intragranular stored energy calculated following the approximation for the dislocation energy given previously[21]. The intragranular stored energy values presented in Fig. 3 were calculated by taking the virgin sample as a reference. It is hard to evaluate the errors involved in the absolute values of the stored energy because an effective procedure to calibrate the method is still lacking, but relative variations of a few percent may be considered as a confidence band. By comparison, we see that the intergranular stored energy is about an order of magnitude smaller than the intragranular type. This is why the intragranular stored energy is usually considered as the full stored energy in heavily deformed materials. However, the most striking feature revealed by our study seems to be the different behaviours of the two types of stored energy during the final stage of the fatigue test. While the intergranular stored energy begins to decrease after the cracks start to propagate (5,506 cycles), the intragranular stored energy continues to grow and slightly decreases only when the sample reaches failure.

Although it is not yet clear whether the observed large intergranular stresses are responsible for the initiation of cracks in fatigued samples, the development of intergranular stress and stored energy determined by neutron diffraction can be directly connected to the microscopic mechanisms of materials damage during fatigue. It is well known that the heterogeneous stress and strain distributions of polycrystalline materials play an important role in crack initiation, crack coalescence, and fatigue lifetime during fatigue deformations[23–28]. Despite arguments about the detailed mechanisms of crack nucleation, the compatibility stresses near grain boundaries caused by different grain orientations are believed to be an important source of failure. It is evident that the average level of the intergranular strain correlates with the amount of the fatigue damage. The increase of the intragranular stored energy observed after crack initiation indicates also that the impingement of slip lines against grain boundaries continues during the crack growth stage, but a competing recovery process could appear in the later stage of fatigue life. More data are needed to obtain a confident description of the stored energy evolution during fatigue. Nevertheless, the ratio between the intergranular and intragranular stored energies can be used for monitoring the fatigue damage of materials with elastic and/or plastic anisotropy.

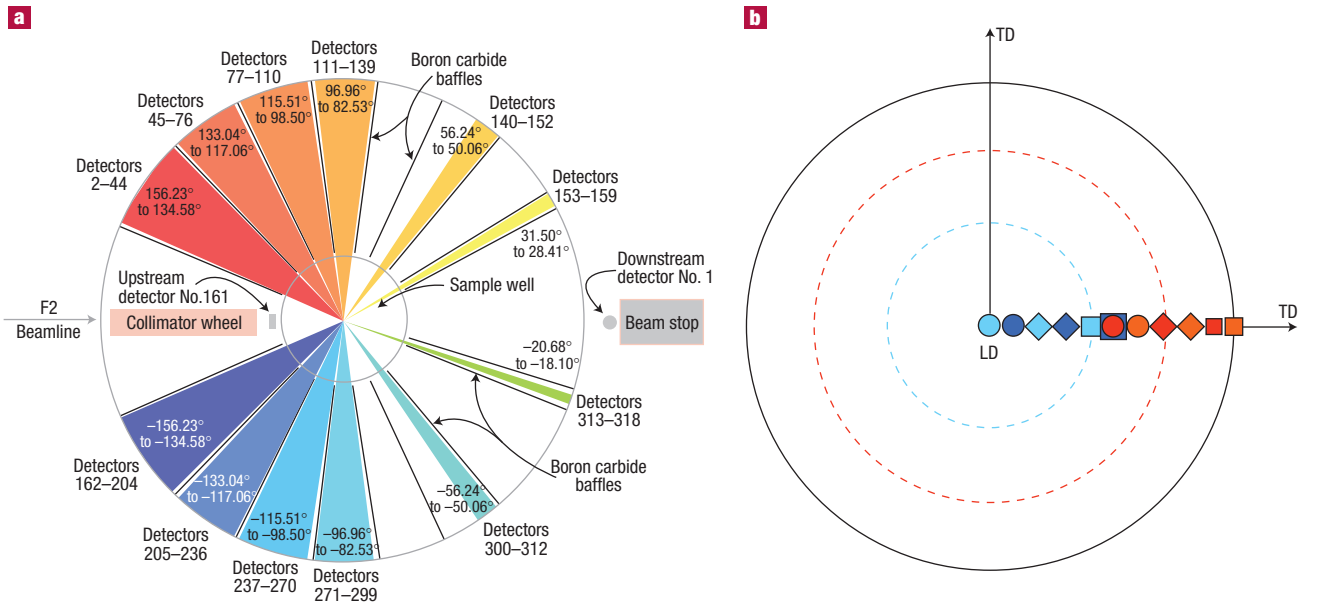

Figure 4 The determination of strain pole figures with a pulsed neutron source. a, The detector layout of the general purpose powder diffractometer at the Intense Pulsed Neutron Source, Argonne National Laboratory, USA. In order to achieve high precision, only high-angle detector banks centered around 144° and 126° were used for the measurements. **b**, Pole figure for a given reflection with the orientations of measured grains marked. The sample was rotated about the ϕ axis in three steps with LD pointing at 27°, 45° and 63° relative to the incident beam in the horizontal scattering plane. In each setting, four orientations were measured as indicated by sets of symbols in the pole figure. The colour of the symbol corresponds to the detector bank with which the measurements were made. The dashed circles indicate the axial symmetry of the sample.

To our knowledge, this is the first time that a correlation between the development of intergranular stress and the material damages during fatigue has been reported. In our view, a detailed characterization of the intergranular stress is an important step for studying the failure mechanism of certain ceramics or natural rocks with a high elastic anisotropy. The experimentally determined intergranular stresses during fatigue should be used as an important reference for the design of advanced materials and the evaluation of fatigue life in traditional engineering materials.

METHODS

The general purpose powder diffractometer (GPPD) is a high-resolution time-of-flight neutron powder diffractometer with a resolution of $\Delta d/d \sim 0.2\%$ for the high-angle detector banks. ^{3}He gas proportional detector tubes are grouped in 12 banks in the horizontal scattering plane, as shown in Fig. 4a[14]. Detectors in each group are used together through electronic time focusing to produce a single diffraction pattern for the detector bank. This gives a resolution of about 10° × 10° for pole figure measurements. The average lattice strain is determined from the diffraction line displacement in neutron time-of-flight. In order to achieve high precision, only high-angle detector banks centred around 144° and 126° were used for the measurements.

A Kappa goniometer was used for the measurement of strain pole figures[14]. The Kappa goniometer was positioned with both the Ω and ϕ axes vertical[29]. The cylindrical specimens were mounted on a microgoniometer attached to the Kappa goniometer head, with their cylindrical axes, which are also the loading direction (LD), in the horizontal scattering plane. The orthogonal direction in the horizontal scattering plane is defined as a transverse direction (TD). During the measurements, the sample was rotated about the ϕ axis in three steps with LD pointing at 27°, 45° and 63° relative to the incident beam in the horizontal scattering plane. Owing to the cylindrical geometry of the sample around LD, three sample positions and four detector banks cover the entire pole figure space, as illustrated in Fig. 4b.

Individual diffraction peaks in the time-of-flight spectrum were fitted separately by convoluting a Voigt sample broadening function with a pulse-shape instrument function[15]. The fitting procedure yields four parameters for each diffraction peak characterizing the peak position, diffraction intensity, integral breadths of gaussian and lorentzian components of the Voigt function[15]. The peak position in time-of-flight is proportional to the average value of the lattice spacing corresponding to a family of {hkl} reflections. The experimental lattice strain was calculated from the change in the peak position relative to the virgin (stress-free) sample. This procedure was applied for each bank separately.

During the construction of SODF, a misfit function, which measures the deviation of the real strain and stress state from the elastic self-consistent state, was used to stabilize the solution of the SODF from the spherical harmonics expansion[8]. Here we considered each grain as a spherical inclusion. The single crystal elastic constants of the stainless steel with C_{11} = 204.6 GPa, C_{12} = 137.7 GPa and C_{44} = 126.2 GPa were used for the calculation.

The estimation of the intragranular stored energy, W_S, follows the general approach considering the dislocation contrast in diffraction[21]. Nevertheless, it is adequate to mention our specific approximation: $W_S = (K/2)\,(\beta_{hkl}^2/C_{hkl})\,F$, where $K = C_{44}/\sqrt{A_i} = 65$ GPa for the stainless steel, $A_i = 2C_{44}/(C_{11} - C_{12}) = 3.77$ is the elastic anisotropy factor, β_{hkl} is the integral breadth for the {hkl} peak, C_{hkl} is the contrast factor, and F is a numerical factor close to 1. In our case, the edge dislocation character gives the following relationship for the contrast factor (data interpolated from ref. 21): $C_{hkl} = 0.327\,[1 - 1.79\,(h^2k^2 + h^2l^2 + k^2l^2)/(h^2 + k^2 + l^2)^2]$, which makes the factor β_{hkl}^2/C_{hkl} almost independent of {hkl} and therefore justifies our assumption for the equation estimating the W_S.

Received 24 October 2002; accepted 9 December 2002; published 19 January 2003.

References

1. Dawson, P., Boyce, D., MacEven, S. & Rogge, R., Residual strain in HY100 polycrystals: comparisons of experiments and simulations. *Metall. Trans. A* **31,** 1543–1555 (2000).
2. Clausen, B., Lorentz, T. & Leffers, T. Self-consistent modelling of the plastic deformation of f.c.c polycrystals and its implications for diffraction measurements of internal stresses. *Acta Mater.* **46,** 3087–3098 (1998).
3. Pang, J. W. L., Holden, T. M. & Mason, T. E. In situ generation of intergranular strains in an Al7050 alloy. *Acta Mater.* **46,** 1503–1518 (1998).
4. Lorentzen, T., Daymond, M. R., Clausen, B. & Tome, C. N. Lattice strain evolution during cyclic loading of stainless steel. *Acta Mater.* **50,** 1627–1638 (2002).
5. Korsunsky, A. M. & James, K. E. Intergranular stress evolution in fcc polycrystals during high cycle fatigue. *ISIS Annual Report* (2001) RB No. 12180. http://www.isis.rl.ac.uk/isis2001.
6. Margulies, L., Winther, G. & Poulsen, H. F. In situ measurement of grain rotation during deformation of polycrystals. *Science* **291,** 2392–2394 (2001).
7. Larson, B. C., Yang, W., Ice, G. E., Budai, J. D. & Tischler, J. Z. Three-dimensional X-ray structural microscopy with submicrometre resolution. *Nature* **415,** 887–890 (2002).
8. Wang, Y. D., Lin Peng, R. & McGreevy, R. L. A novel method for constructing the mean field of grain-orientation-dependent residual stress. *Phil. Mag. Lett.* **81,** 153 –163 (2001).
9. Wang, Y. D., Lin Peng, R., Wang, X.-L. & McGreevy, R. L. Grain-orientation-dependent residual stress and the effect of annealing in cold-rolled stainless steel. *Acta Mater.* **50,** 1717–1734 (2002).
10. Behnken, H. Strain-function method for the direct evaluation of intergranular strains and stresses. *Phys. Status Solidi A* **177,** 401–418 (2000).
11. Mansur, L. K., Gabriel, T. A., Haines, J. R. & Lousteau, D. C. R&D for the Spallation Neutron Source mercury target. *J. Nucl. Mater.* **296,** 1–16 (2001).
12. Tian, H. *et al.* Influence of mercury environment on the fatigue behaviour of spallation neutron source (SNS) target container materials. *Mater. Sci. Eng.* **314,** 140–149 (2001).
13. Strizak, J. P., DiStefano, J. R., Liaw, P. K. & Tian, H. The effect of mercury on the fatigue behaviour of 316 LN stainless steel. *J. Nucl. Mater.* **296,** 225–230 (2001).

14. http://www.pns.anl.gov/instruments/gppd/
15. Wang, Y. D., Wang, X.-L., Stoica, A. D., Richardson, J. W. & Lin Peng, R. Determination of the stress orientation distribution function using pulsed neutron sources. *J. Appl. Cryst.* **36,** 14–22 (2003).
16. Quesnel, D. J. & Meshii, M. The response of high-strength low alloy steel to cyclic plastic deformation. *Mater. Sci. Eng.* **30,** 223–241 (1977).
17. Quesnel, D. J., Meshii, M. & Cohen, J. B. Residual stresses in high strength low alloy steel during low cycle fatigue. *Mater. Sci. Eng.* **36,** 207–215 (1978).
18. Noyan, I. C. & Cohen, J. B. X-ray-diffraction study of changes in stress-strain distributions during the fatigue of a 2-phase alloy. *Mater. Sci. Eng.* **79,** 149–155 (1986).
19. Winholtz, R. A. & Cohen, J. B. Changes in the macrostresses and microstresses in steel with fatigue. *Mater. Sci. Eng. A* **154,** 155–163 (1992).
20. Holden, T. M., Holt, R. A. & Clarke, A. P. Intergranular stresses in Incoloy-800. *J. Neutron Res.* **5,** 241–264 (1997).
21. Borbely, A., Driver, J. H. & Ungar, T. An X-ray method for the determination of stored energy in texture components of deformed metals; application to cold worked ultra high purity iron. *Acta Mater.* **48,** 2005–2016 (2000).
22. Ungar, T., Dragomir, I., Revesz, A. & Borbely, A. The contrast factors of dislocations in cubic crystals: the dislocation model of strain anisotropy in practice. *J. Appl. Cryst.* **32,** 992–1002 (1999).
23. Laird, C. in *Physical Metallurgy* vol. 3 (eds Cahn R. W. & Haasen P.) 2293–2397 (Elsevier Science, Amsterdam, 1996).
24. Suresh, S. *Fatigue of Materials* (Cambridge Univ. Press, Cambridge, 1998).
25. Guiu, F. & Dulniak, R. On the nucleation of fatigue cracks in pure polycrystalline α-iron. *Fatigue Fract. Eng. Mater. Struct.* **5,** 311–321 (1982).
26. Pommier, S. 'Arching' effect in elastic polycrystals: implications for the variability of fatigue lives. *Fatigue Fract. Eng. Mater. Struct.* **25,** 331–348 (2002).
27. Le Biavant, K., Pommier, S. & Prioul, C. Local texture and fatigue initiation in a Ti-6Al-4V titanium alloy. *Fatigue Fract. Eng. Mater. Struct.* **25,** 527–545 (2002).
28. Zhang, Y. & Jiang, Q. Twinning-induced stress and electric field concentrations in ferroelectric ceramics. *J. Am. Ceram. Soc.* **78,** 3290–3296 (1995).
29. Wang, X.-L., Wang, Y. D. & Richardson, J. W. Experimental error caused by sample displacement in time-of-flight neutron diffractometery. *J. Appl. Cryst.* **35,** 533–537 (2002).

Acknowledgements

We thank E. Maxey for assistance in the experiment. This research was sponsored by the US Department of Energy, Division of Materials Sciences and Engineering, under Contract DE-AC05-00OR22725 with Oak Ridge National Laboratory managed by UT-Battelle. The neutron diffraction work has benefitted from the use of the Intense Pulsed Neutron Source at Argonne National Laboratory, which is funded by the US Department of Energy, BES-Materials Science, under Contract No. W-31-109-ENG-38. This research was also supported in part by an appointment to the Oak Ridge National Laboratory Postdoctoral Research Associates Program administered by the Oak Ridge Institute for Science and Education, and by the US National Science Foundation, the Combined Research and Curriculum Development (CRCD) Program, under EEC-9527527, with M. Poats as the contract monitor, and the Integrative Graduate Education and Research Training (IGERT) Program, under DGE-9987548, with W. Jennings and L. Goldberg as contract monitors. HT and PKL thank L. Mansur and J. Strizak of the Oak Ridge National Laboratory for their kind support of HT's Ph.D. thesis research related to fatigue behaviour of Type 316 stainless steel for the application of the target container materials of the Spallation Neutron Source.
Correspondence and requests for materials should be addressed to Y.W. and X.W.

Competing interests statement

The authors declare that they have no competing financial interests.